

**Investigation of Hot Cracking Phenomena in Light-Weight Armor  
Steel Based on the FeMnAl-C Alloy System**

**William Evans**  
**Antonio J. Ramirez, Ph.D.**  
Department of Welding Engineering  
The Ohio State University  
Columbus, OH

**Katherine Sebeck, Ph.D.**  
US Army TARDEC  
Warren, MI

**Abstract**

*The US Army TARDEC has been researching an alternative to current armor steel that is both tough, and light-weight. The studied alloy is based on the Fe-Mn-Al-C system. This study was conducted to investigate and quantify this alloy's susceptibility to hot cracking phenomena related to casting and welding. Very little research has been done on general weldability of this alloy system, so the results of these tests will be compared to other high Mn steels, and alloys that have undergone cast pin tear testing. Testing will be conducted utilizing button melting tests, autogenous spot welds, and cast pin tear testing. The cast pin tear testing was conducted to measure this alloys susceptibility to weld solidification cracking. The spot welds were used to quantify the susceptibility of the weld heat affected zone (HAZ) to liquation cracking, as well as to observe the solidification structure of the fusion zone. The testing results showed that the FeMnAl system in its current form has a susceptibility to both solidification cracking and to HAZ liquation cracking.*

**Introduction**

*Material Background*

FeMnAl is a family of age hardenable steels based on the Fe-Mn-Al ternary system. This material was derived initially from high Mn steels called Hadfield steels [1]. These steels are used extensively in the rail road industry and are known for their work hardenability, and wear resistance [1]. FeMnAl has been

previously researched by the Navy in the 1950's in hope of finding an alternative to expensive Ni/Cr containing stainless steels, and this has been the main driving force for the development of the FeMnAl alloys through the late 20<sup>th</sup> century [2-3]. In more recent years, FeMnAl has been researched as a candidate for an advanced high strength steel (AHSS) in thin sheet applications [4-6]. Its reduction in density and combination of high strength and ductility make it a good

candidate for transportation applications. In previous literature, FeMnAl alloys have reported tensile strength from 600-2000 MPa, with elongations to failure peaking around 70% [2 ,4-6]. In the peak aged condition, elongation to failure is between 30-40% [2].

*Microstructure and Age hardening*

FeMnAl alloys solidify as FCC - (gamma) austenite and can transform into small amounts of (alpha) ferrite at the end of solidification. These alloys can also form (kappa) – carbides, and (Beta)-Mn phases. The carbides act as an age hardening precipitate, while (beta) phases can be deleterious to mechanical properties, and should be avoided [2, 7-9].

Carbide precipitation follows a classical age-hardening reaction [2]. In which, precipitates can be coarsened to a peak-aged condition, usually exchanging ductility for strength. Therefore, there are several procedures that can be conducted to tailor the properties of this alloy system. It has been reported that for maximum ductility and toughness, the heat treatment should aim for the largest volume fraction of austenite. An age hardening curve for a FeMnAl alloy is displayed below in Figure 1 [2].

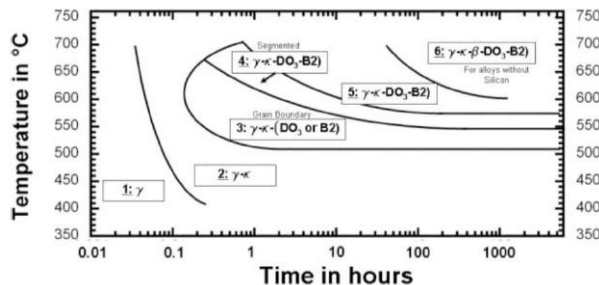


**Figure 1:** Time temperature transformation curves for 1.25 wt.% Si FeMnAl alloy

*New Class of Armor Steel*

Recently the U.S. Army has been conducting research on the manufacturability of FeMnAl for thick plate armor steel applications [10]. This current research is based on studies conducted in 1979, and is examining both cast and wrought plate. The hope is to create a steel that will fit as a Class V rolled Homogeneous Armor (RHA) under MIL – DTL 12560.

Current research has found that conventional steel making procedures can be utilized to cast FeMnAl using both open air and vacuum furnaces to produce this steel [10]. Through the high additions of Al and Si, the liquidus temperature of the material has been reduced to similar temperatures of Cast Iron [10].

In addition to common casting procedures this alloy system can also be conventionally cut and machined [10]. It has been recommended to utilize carbide tipped cutting tools, and band-saw blades, as well as powder injection processes for flame cutting.

A heat of wrought material with a similar composition to the cast material being investigated in the study has shown, through ballistics testing, to be a promising candidate for a direct replacement for RHA steels used today [10]. Additionally, the density of the FeMnAl wrought plate was measured to be 13% less than RHA [10]. So the hope is that without changing the geometries or design of current armor vehicles FeMnAl can be utilized for direct weight savings, at no cost to the armor’s performance. Further testing and analysis is needed to prove that this substitution is feasible.

*Hot Cracking in Metals*

Hot cracking refers to a family of defects that may occur in metals at elevated temperatures, and are always associated with the presence of liquid, or liquid films [11]. The liquid films are found at grain boundaries, and exhibit no strength. Upon seeing an elevated stress level these liquid films “open up” to form cracks. Their size can vary greatly from fine cracks, to extremely large cracks visible with the naked eye.

In welding, the types of hot cracking that have been studied are weld solidification cracking, and weld heat affected zone liquation cracking [11]. Weld solidification cracking is analogous to hot tearing in castings, and refers to cracks associated with the presence of liquid films at solidification grain boundaries at the end of solidification.

The metal alloys most associated with this form of cracking are those that solidify as a FCC structure, and those with low melting second phases, or eutectic reactions [11].

### Cast Pin Tear Testing

Cast Pin Tear Testings was invented by Hull in the 1960’s and was used to measure the hot tearing response of alloys used for casting [12]. In the past decade Ohio State has redeveloped this test for solidification cracking measurements. The test is currently in its third generation, and has been used extensively to measure the cracking response of stainless steels, carbon steels, and Ni- base alloys [13].

The test involves levitation melting a charge of material, then dropping it into a pin mold. The pin molds have been designed to allow for a stress riser at the top of the pin. As the pin length increases more stresses build up at the end of solidification which leads to solidification cracking. The stresses

exhibited on the pins is purely due to the solidification behavior, and material shrinkage of the alloy being tested.

This test allows for the response of an alloy to be compared to other alloys with known susceptibilities [13]. The average percentage of the circumference which is covered in cracks is reported versus the length of the pin. An example graph is shown in Figure 2. This test is good for comparing different heats of material, and new experimental alloys because it utilizes much less material compared to other weldability tests.

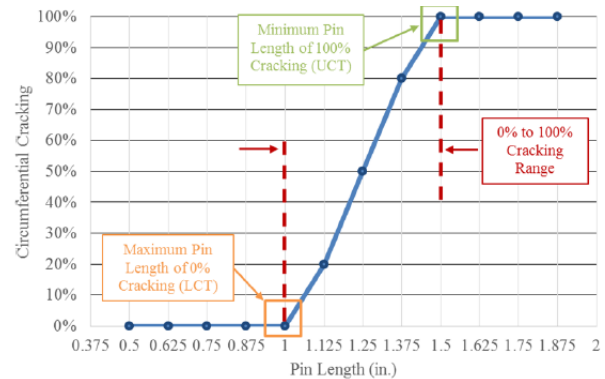


**Figure 2:** CPTT average cracking response curve labeled with ranking criteria

To date, little research has been conducted on the weldability, and cracking response of this material during fabrication. The purpose of this study was to investigate the FeMnAl alloy’s susceptibility to these forms of cracking, and to study any defects associated with fabrication.

## Experimental Procedure

### Material Used

Material was acquired from U.S. Army TARDEC in ½ inch thick plates. The plates were cast material in the as cast condition. The material composition is displayed below in Table 1. It should be noted that the

composition for cast FeMnAl exhibits a higher level of Si when compared to the wrought material being studied. This higher level of Si is to increase fluidity for pouring cast material.

**Table 1:** Fe-Mn-Al-C composition used for CPTT

Fe	Al	C	Cu	Mn	Mo
Bal.	8.95	0.98	0.031	29.9	0.51
Ni	P	S	Si	Ti	
0.01	0.0022	0.003	1.13	0.002	

*Initial Study*

To simulate a weld fusion zone, and a weld HAZ, a small piece of material was sectioned from the cast plates and a melt pool was created using a GTA spot weld. The melt pool was created on a cleaned face of the material, and was cross sectioned for optical microscopy.



**Figure 3:** GTA spot welding set up with an image of the sample spot weld in the lower left corner

In addition to a melt pool analysis, some material was melted using OSU’s button melting system. The button melting system is utilized to simulate an equilibrium solidification condition. The button melting system consists of a water cooled copper

crucible contained within an argon purged chamber. The melting is done by inserting a GTA torch into the chamber and using an arc to fully melt the material charge. The buttons of material were made by sectioning pieces of material from the cast plate, cleaning the material, and then inserting them into the melt chamber. The button was then cross sectioned and examined using optical microscopy.

*CPTT Study*

The CPTT was conducted in similar fashion to previous studies conducted at OSU. The main example being work conducted on high Mn steels conducted by M. Orr [14]. A schematic of the testing apparatus is shown below in Figure 4.

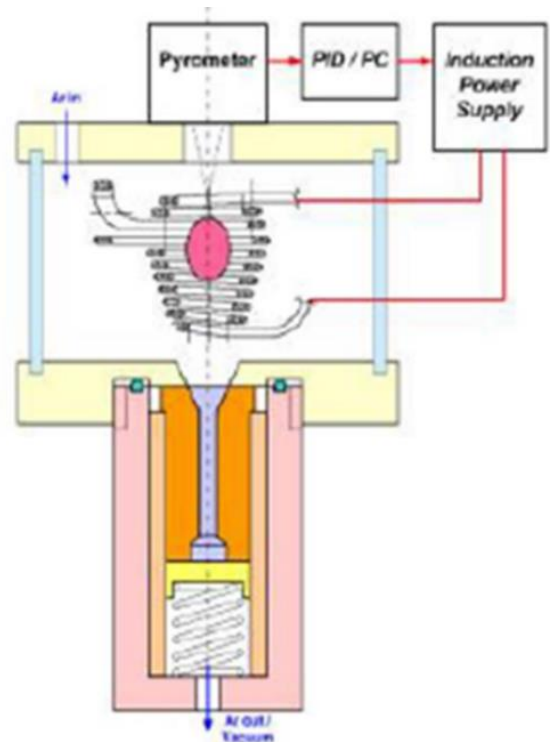


**Figure 4:** Schematic of the cast pin tear testing apparatus

The procedure for conducting a CPTT is to first weigh out the samples that is intended to be tested, this allows the operator to know how much material is in the cast pin, as well

as what size cast pin mold can be used. Once weighed, the material can be cleaned and prepared for button melting. The material is then melted into a button like the procedure described previously. A melt button is preferred for the initial charge in the CPTT apparatus because it provides a uniform shape, and a homogenized composition. The button is then cleaned and inserted into the induction coil where a quartz funnel is located to direct the molten charge into the mold. The mold shown in figure 5 is attached to the bottom of the melt chamber in an aluminum holder, which is spring loaded to allow easy removal of the pin mold. The melt chamber can then be sealed, and argon is pumped into the chamber to create an inert environment. The pin mold holder is also designed so that the argon can flow into it as well. Once an atmosphere purging cycle is completed, the charge is levitation melted using the induction coil unit. A pyrometer is attached to the apparatus and relays the temperature of the charge of material back to the testing program, and upon reaching a set temperature the induction unit is switched off, and the material is dropped into the mold for casting. The temperature set on the testing program changes per material, but is usually set to 50 degrees above the melting temperature. In this case a temperature of 1450 degrees Celsius was utilized.



Figure 5: Example of CPTT pin mold

When dropped into the mold the material will begin to solidify from the bottom of the mold to the top. Located at the top of the mold is a stress riser which is intended to create a region in the pin where an adequate level of stress is created to induce solidification cracking.

Due to the fact that this material has a high level of Mn, some challenges were presented for this particular weldability test. Primarily, the pyrometer feedback system was impeded by the high vaporization level of Mn. The vaporized Mn created a thin layer of soot which impeded the sensor's ability to gather an accurate temperature reading. As a result, each test had to be manually cast, which allows for variability in casting temperatures.

#### *Cast Pin Analysis*

Each cast pin was first examined to ensure that no casting defects were present in the pin before further analysis. These casting defects can occur for several reasons, from cleanliness of the charge of material, cleanliness of the casting mold, casting temperature, and cleanliness of the casting chamber. For this reason, it was important to clean all aspects of the apparatus before use.

After determining that each pin was viable for reporting, the pins were examined under a binocular microscope for any solidification cracks that occurred. If any cracks were encountered the percent cracking was measured. The percentage of cracking refers to how much of the 360 degrees of pin was covered in cracking. This cracking percentage is then plotted on the y-axis of a chart with pin length on the x-axis. An example of this chart was shown in Figure 2. These charts can be used to determine the cracking threshold of any given material. Once a set of data is generated then a

comparison can be made to other materials tested in this way. For this study a minimum of 3 defect free pins from each pin length were used to comprise the data set presented.

## Results and Discussion

### *Initial Testing*

The initial cast structure investigated using OSU's button melting system is shown in Figure 6. The microstructure reveals a fully FCC matrix, with interdendritic ferrite, and carbide "peppering" throughout the matrix. This structure is very similar to the cast microstructure seen by Howell et. al. [2]. No additional processing steps were taken on this sample. Segregation of the ferrite phase was well dispersed in the center of the button, but was more concentrated towards the edges.

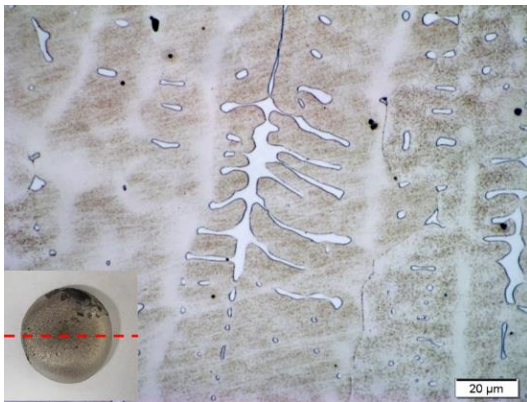


**Figure 6:** Micrograph of FeMnAl cast button microstructure. The matrix is austenitic FCC, and the light region is interdendritic Ferrite. An image of the as cast button before sectioning is shown in the lower left hand corner

The autogenous weld fusion zone (Figure 7) created using a GTA spot weld revealed a similar solidification structure as observed in the melt button. Significant segregation of the interdendritic ferrite was also observed in the fusion zone. A small crater was observed at the top of the weld, this was most likely caused by material shrinkage during solidification. The weld HAZ exhibited grain growth, with ferrite along the grain

boundaries. Several cracks appeared in the coarse grain HAZ, and the partially melted zone of the HAZ. These cracks are most likely HAZ liquation cracks which was associated with the interdendritic ferrite that segregated to the grain boundaries. This is evident from what appears to be ferrite scattered along the cracks. It is theorized that the liquidus temperature of the ferrite has been reduced due to the segregation of Al into the alpha ferrite phase during solidification. This needs to be confirmed through additional chemical analysis, and additional computer simulation. No solidification cracks were exhibited in the cast button sample, but the presence of a crater, and a high level of interdendritic phases in an FCC matrix can give evidence to a susceptibility to this cracking phenomenon.

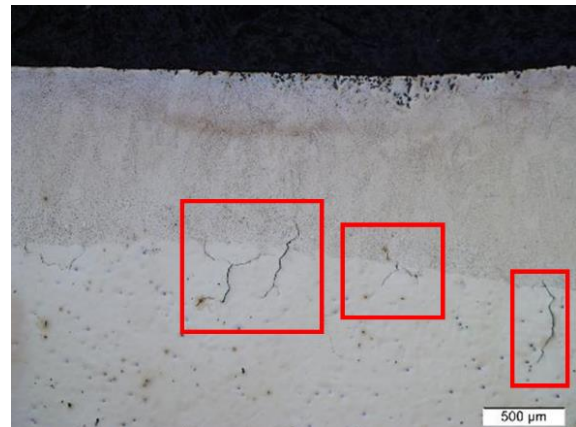


**Figure 7:** Cross section of autogenous spot weld. HAZ liquation cracks are highlighted in the CGHAZ extending into the fusion zone

### *Cast Pin Tear Testing*

Testing was conducted on two different heats of material provided to OSU from TARDEC, all initial testing and the first round of CPTT was conducted on the first heat. The second heat was designated for just cast pin tear testing use. The first round of testing was not complete enough for good statistical data, but was conducted to see the

initial response of the material. During the initial testing cracking did not occur until 1.375 in pins, and then no cracking occurred again until 1.75 in pin lengths. Above 1.75 in cracking occurred in every pin. Not enough pins were taken to fully report the response of the first material, but results appeared promising.

The second round of CPTT was conducted to get a complete response of the material, this means that several pins were taken at each length in an attempt to attain several defect free pins. The high Mn content of the FeMnAl made it difficult to get clean defect free pins, an example of a pin with and without defects is displayed in Figure 8. The high vaporization of Mn leads to difficulty in controlling the casting temperature of the charge. This makes the repeatability of the test difficult. Below in Table 2, and Figure 9 is the data from this round of testing. The table displays a list of the pin lengths tested, and the average percent cracking in the respective pins. Figure 9 shows a plot of pin length versus cracking percent.



**Figure 8:** Image of two sample 1 inch pins. One pin exhibits cracking due to a casting defect, and the other is an ideal cast pin.

**Table 2:** Pin length versus percent cracking for CPTT

Pin Length (in)	Percent Cracking
0.75	0
0.875	0
1	22
1.125	10
1.25	64
1.375	88
1.5	100
1.75	65

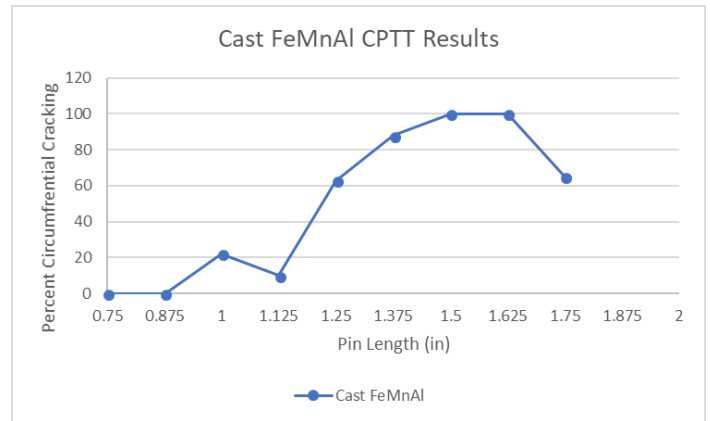


**Figure 9:** FeMnAl CPTT results exhibiting average crack percentage versus pin length

No observable cracking occurred in pin lengths under 1 in. At 1 inch several small cracks occurred on the surface, these cracks are displayed in Figure 10. Similar cracks were seen at 1.125 inch, and 1.25 in pins. Macroscopic cracks that could be observed with the naked eye were not observed until 1.5inch pins. Above 1.5 inches large cracks were seen in all samples. Images of cracking observed in these pins is shown in Figure 11. From these observations a pin length of 1 inch was determined to be the LCT of this alloy.

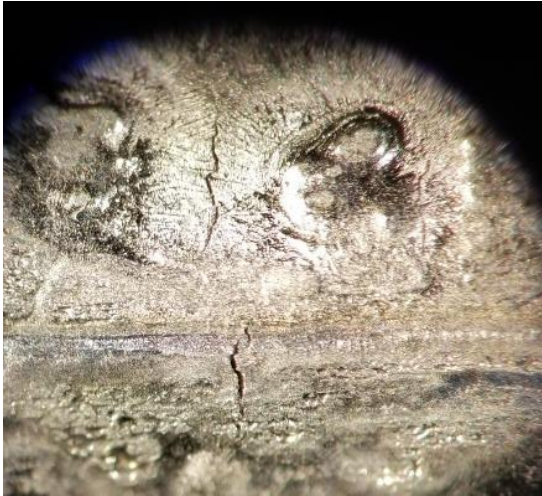


Figure 10: Image of solidification cracks in a 1 inch cast pin



Figure 11: Examples of cracking in 1.375 inch and 1.5 inch cast pin

This data can be compared to other cast pin tear testing results previously done at OSU. Figure 12 displays data presented in two thesis studies conducted at OSU, which utilized CPTT on two different materials. The first study was conducted by M. Orr [14], who studied the cracking response of different heats of Ni-base filler metal FM-82. The two heats are broken down into an alloy with a “good” cracking response, and the second heat exhibits a “poor” cracking response. The second study was conducted by J. Lenzo [15], who was examining the

cracking response of high Mn steels. The exact composition of these alloys is not known due to the proprietary nature of this study, but the response of the alloy with additions of B and W was studied. Displayed in this figure are only the base compositions, this is due to the fact that the cast FeMnAl utilized in this study had no additions of W or B. These Mn steels exhibited fully FCC solidification, and showed some similarities to FeMnAl. While these two examples are not perfect examples of materials similar to FeMnAl, the cracking responses can be compared to one another using these CPTT testing methods.

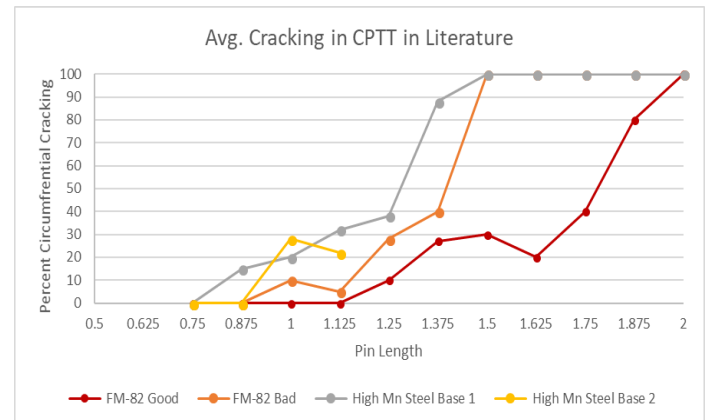
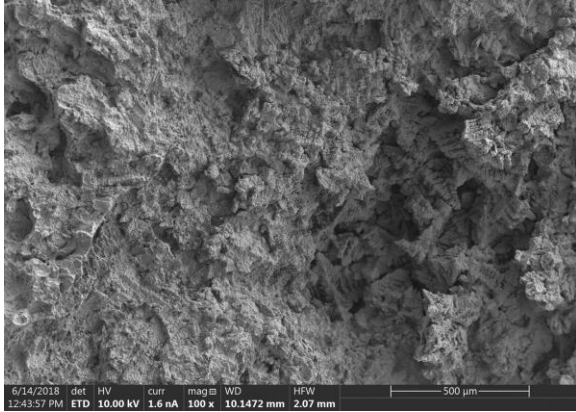


Figure 12 CPTT results shown in two thesis studies conducted at OSU by M. Orr, and J. Lenzo. The cracking response is shown for FM-82, and High Mn steels.

### Fracture Surfaces

Fractography was conducted on several of the cast pins that exhibited catastrophic failure, and a good example of the fracture surfaces observed is shown in Figure 16, and Figure 17. This fracture surface exhibits an example of a dendritic fracture mode which is common in solidification cracks. The solidification dendrites are quite apparent, and there is evidence of liquid films along the tips of the dendrites. This evidence points to a failure due to solidification cracking.



**Figure 13** Fracture surface exhibiting solidification cracking taken from a 1.5 inch pin that exhibited catastrophic failure.

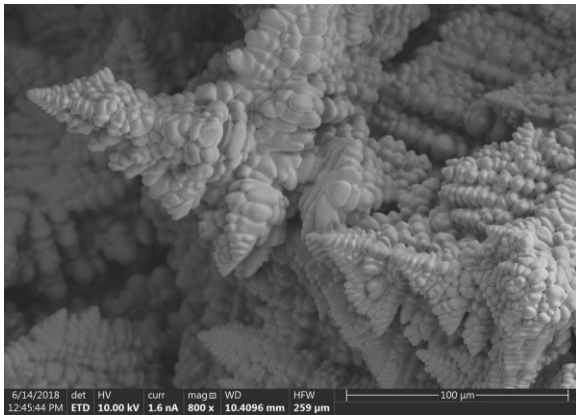


**Figure 14** Higher magnification view of fracture surface exhibiting solidification cracking taken from a 1.5 inch pin that exhibited catastrophic failure.

## Conclusions

As stated earlier, due to a lack of similar materials to FeMnAl being tested using the CPTT method, it is challenging to reach broad conclusions about this family of materials. However, with regard to the overall susceptibility to solidification cracking, a few conclusions regarding the specific heat tested can be drawn.

1. Solidification cracking was observed in several cast pins, this was confirmed by observing the fracture surfaces of failed pins.
2. When comparing this study's results to a previous study conducted on two Ni-base

FM one with favorable cracking resistance and the other a high susceptibility the FeMnAl is ranked between the two [14].

3. Compared to the other high Mn steels tested by J. Lenzo FeMnAl exhibits a cracking response similar to the base unaltered steel, but has a higher lower cracking threshold. These Mn steels were labeled as having poor cracking responses to solidification cracking [15].
4. The main takeaway from these results are that this particular composition of cast FeMnAl will exhibit a susceptibility to solidification cracking given the correct stress levels at the end of solidification. This will need to be kept in mind for future casting development, and future filler metal development.
5. With regard to the initial autogenous weldments, a high susceptibility to HAZ liquation cracking was observed with the given parameters used for the weldment. For future welding development and future hot rolling efforts, this will require special consideration.

Further CPTT is required on different compositions of materials to fully understand the cracking response FeMnAl base alloys. In conjunction to CPTT additional weldability tests to are needed confirm the results of these tests.

## References

1. Hadfield, R., Burnham, T. H., "Special Steels", 2nd ed., p.100, The Pitman Press, New York (1933).
2. Ham, J. L., Cairns, R. E., "Manganese Joins Aluminum to Give Strong Stainless,"Product Engineering, Dec, pp. 51-52 (1958).

3. Howell, Ryan A., "Microstructural influence on dynamic properties of age hardenable FeMnAl alloys" (2009). Doctoral Dissertations. Paper 1940.
4. Yinghua Jiang and Chunqian Xie 2017 IOP Conf. Ser.: Mater. Sci. Eng. 207012053
5. Fuqiang Yang, Renbo Song, Yaping Li, Ting Sun, Kaikun Wang, Tensile deformation of low density duplex Fe–Mn–Al–C steel, *Materials & Design*, Volume 76, 2015, Pages 32-39, ISSN 0261-3069.
6. Zhang, X., Yang, H., Leng, D., Zhang, L., Huang, Z., & Chen, G. (2016). Tensile Deformation Behavior of Fe-Mn-Al-C Low Density Steels. *Journal of Iron and Steel Research, International*, 2016(23(9)), 963-972. Retrieved May 18, 2018.
7. Fatma Hadeif, Solid-state reactions during mechanical alloying of ternary Fe–Al–X (X=Ni, Mn, Cu, Ti, Cr, B, Si) systems: A review, *Journal of Magnetism and Magnetic Materials*, Volume 419, 2016, Pages 105-118, ISSN 0304-8853.
8. Liu, J., Chen, W., Jiang, Z., Liu, L., & Fu, Z. (2017). Microstructure and mechanical properties of an Fe-20Mn-11Al-1.8C-5Cr alloy prepared by powder metallurgy. *Vacuum*, 137, 183-190. doi:10.1016/j.vacuum.2016.12.039
9. Chen, S., Rana, R., Haldar, A., & Ray, R. K. (2017). Current state of Fe-Mn-Al-C low density steels. *Progress in Materials Science*, 89, 345-391. doi:10.1016/j.pmatsci.2017.05.002
10. Howell, R. and Gerth, R., "Fe-Mn-Al-C Alloy Steels – A New Armor Class," SAE Technical Paper 2017-01-1703, 2017, doi:10.4271/2017-01-1703.
11. Lippold, J. C. (2015). *Welding metallurgy and weldability*. Hoboken: John Wiley & Sons.
12. F. C. Hull, "Cast-Pin Tear Test for Susceptibility to Hot Cracking," *Welding Journal*, vol. 38, pp. 176-179, 1959.
13. T. Luskin, Master's Thesis: Investigation of Weldability in High-Cr Ni-base Filler Metals, Columbus, OH, 2013.
14. Orr, M. R., & Lippold, J. C. (2016). Solidification cracking performance and metallurgical analysis of filler metal 82 (Unpublished master's thesis). The Ohio State University.
15. Lenzo, J. C., & Lippold, J. C. (2016). Evaluation of the effect of tungsten and boron additions on the microstructure and solidification cracking susceptibility of Fe-Mn-C filler metals. The Ohio State University